

How to Implement Synthetic Diagnostics in the BOUT++ Framework

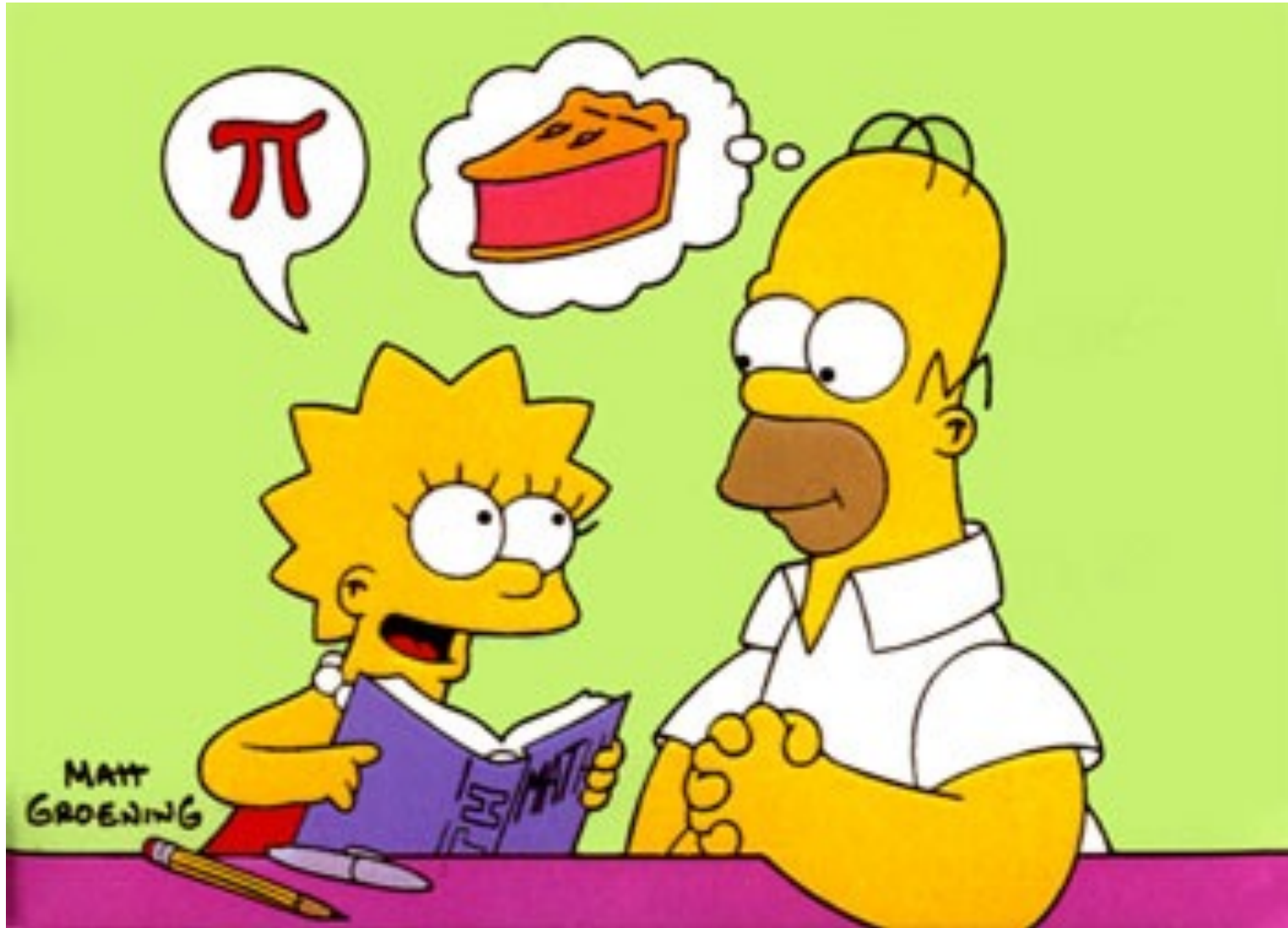
C. Holland, UCSD

BOUT++ 2013 Workshop

September 3-6, 2013 @ Livermore LLNL

UC San Diego

AKA translating simulation to experiment



Two bits of wisdom(?) to keep in mind

“[A]ll models are wrong, but some are useful”

George E. P. Box

“Nobody believes the simulation except the person who did it,
everybody believes the experiment except the person who did it”

Ancient CFD community proverb

(see. A. Einstein for original theory vs. experimental proverb)

Synthetic Diagnostics Essential Component of Quantitative Code-Experiment Comparisons

- Need to compare predictions of turbulence characteristics, not just equilibrium profiles/fluxes, in order to build confidence in underlying physics models implemented in a given code
 - Building this confidence is essential if we want to extrapolate to future devices
- In order to do ~~“apples-to-apples”~~ “pi-to-pi” comparisons of simulation and experiment, need to not just model the turbulence, but also how a given diagnostic “sees” the turbulence
- This is done by creating a synthetic diagnostic which attempts to reproduce what the diagnostic would have seen had it observed the simulation fluctuations
- Two common components to a synthetic diagnostic:
 - Accounting for spatiotemporal sensitivities: finite integration areas, times, sampling rates, wavenumber sensitivities, etc.
 - Accounting for differences between simulation quantities (δn_e , $e\delta\phi/T_e$, δT_e etc.) and measured quantities (I_{sat} , V_{float} , δI etc.)

Outline: “worked” example for two core turbulence synthetic diagnostics using GYRO data

- Aim of this talk is to provide a concise overview of how one practically implements synthetic diagnostics, using the synthetic Beam Emission Spectroscopy (BES) and Correlation Electron Cyclotron Emission (CECE) diagnostics developed for core turbulence as examples
- Procedure for adapting to BOUT (or other codes) should be direct and clear at the end of the talk
- Will also quickly go over relevant bits of signal processing for calculating spectra and end with a few quick examples of edge-relevant synthetic diagnostic studies

Code-Experiment Turbulence Comparisons Should Always be Based on Statistical Analysis

- Basis for most code-code and code-experiment comparisons is various spectral power densities (and closely related coherency and cross-phase) calculated from a time window much longer than characteristic turbulence times (e.g. correlation times)
- The spectral approach is most appropriate/useful when turbulence saturates about some stationary average intensity
- If nonlinear state is highly intermittent or bursty, characterization via other measures such as probability distribution function are likely to be more useful than simple spectral analyses

Signal Processing and Statistical Analysis Literature Have Well-Defined Formulas for Accurately Calculating Measures and Their Uncertainties- Use Them!

- Two useful examples:
 - E. J. Powers, J. Y. Hong, Ch. P. Ritz, “**Applied Digital Time Series Analysis**”
 - J. S. Bendat and A. G. Piersol, “**Random Data Analysis and Measurement Procedures**”
- **Key idea:** break entire time record into N subsegments, use ensemble statistics of spectra calculated from subsegments to calculate best estimates of mean and variance.
- E.g. for cross-spectrum $\mathbf{S}_{xy}(\mathbf{f}) = \langle \mathbf{X}^*(\mathbf{f})\mathbf{Y}(\mathbf{f}) \rangle$, generally quote results as

$$S_{xy}(f) = \hat{S}_{xy}(f) \pm \sqrt{\text{var}(\hat{S}_{xy})} \quad \text{where}$$

$$\hat{S}_{xy} = \frac{1}{N} \sum_{i=1}^N X_i^*(f) Y_i(f) \quad \text{var}(\hat{S}_{xy}) = \frac{1}{N} S_{xx}(f) S_{yy}(f) \{1 - \gamma_{xy}^2(f)\} \quad \hat{\gamma}_{xy}^2(f) = \frac{|\hat{S}_{xy}|^2}{\hat{S}_{xx} \hat{S}_{yy}}$$

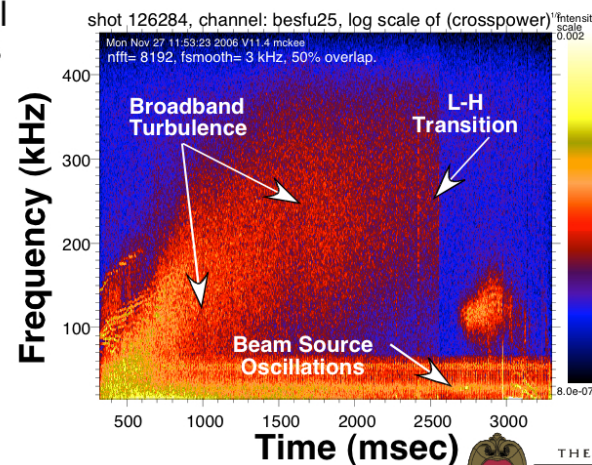
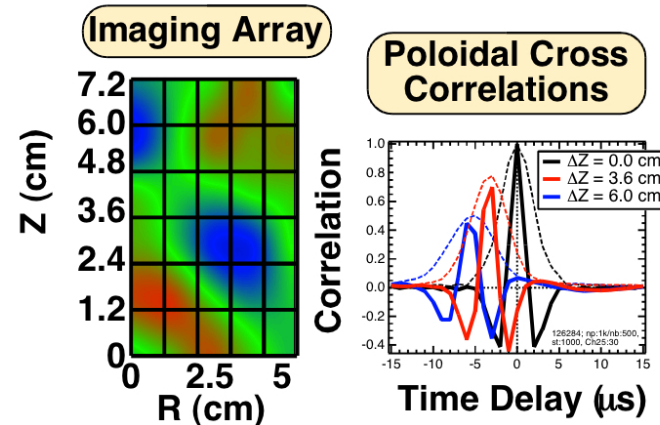
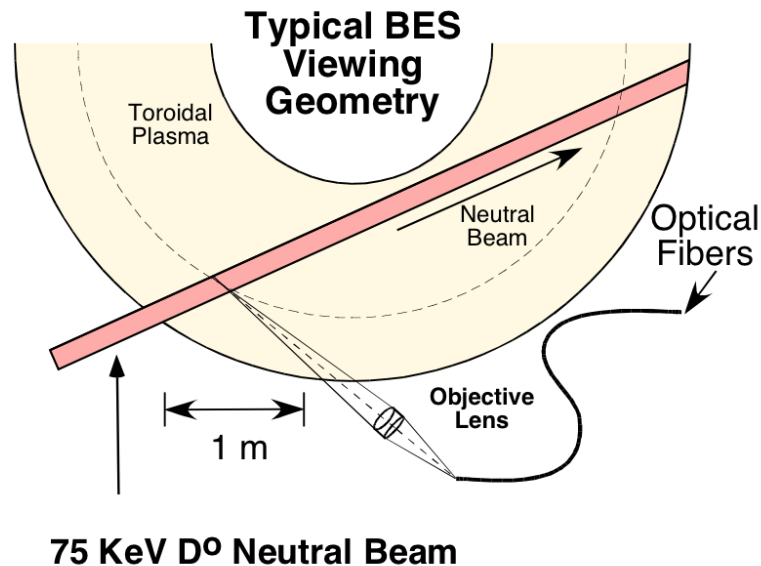
Example: synthetic BES & CECE

BEAM EMISSION SPECTROSCOPY MEASURES SPATIALLY LOCALIZED, LONG-WAVELENGTH ($k_{\perp}\rho_i < 1$) DENSITY FLUCTUATIONS

Collisionally-excited, Doppler-shifted neutral beam fluorescence

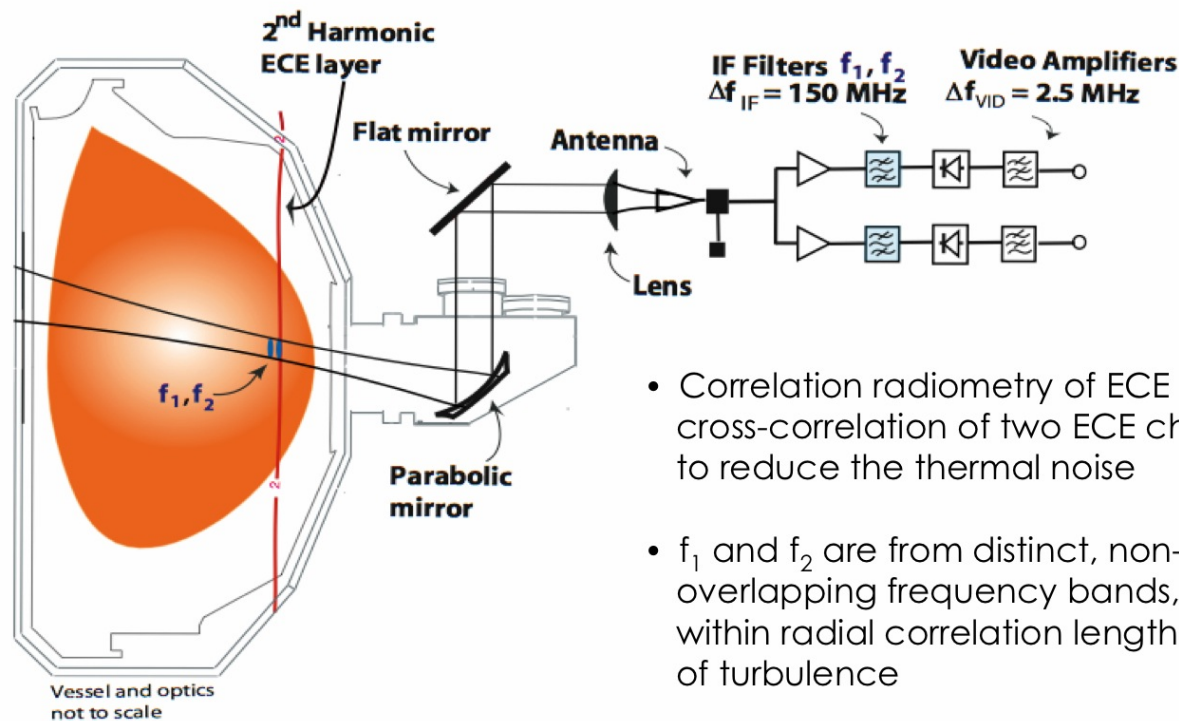
$$D^0 + e, i \Rightarrow (D^0)^* \Rightarrow D^0 + \gamma(n=3 \rightarrow 2, \lambda_o = 656.1 \text{ nm})$$

Emission intensity proportional to local density



Example: synthetic BES & CECE

Correlation Electron Cyclotron Emission (CECE) Diagnostic Measures Local, Low-k Electron Temperature Fluctuations



- Correlation radiometry of ECE uses cross-correlation of two ECE channels to reduce the thermal noise
- f_1 and f_2 are from distinct, non-overlapping frequency bands, within radial correlation length of turbulence
- Measure RMS amplitude and power spectrum, T_e/T_e



TEXT (Cima 1995)
W7-AS (Sattler 1994)
DIII-D (White 2007)

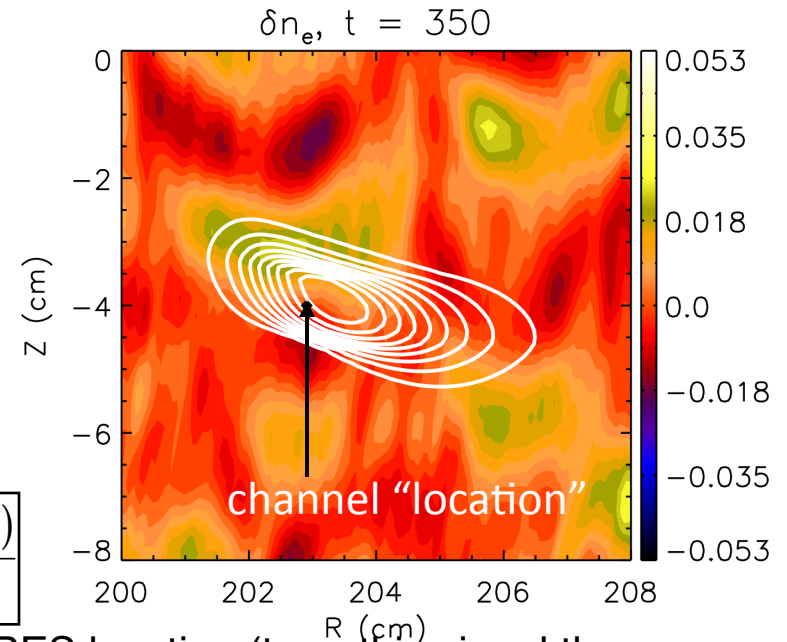
Ex: Applying BES PSF to GYRO Simulation Data

- IDL post processing tool written to generate synthetic BES array; PSF form taken from calculation by M. Shafer
- Tool first interpolates PSF data (generated on a regularly spaced (R,Z) grid) onto a grid compatible with GYRO data (which uses a field-line following (r,θ,α) coordinate system)

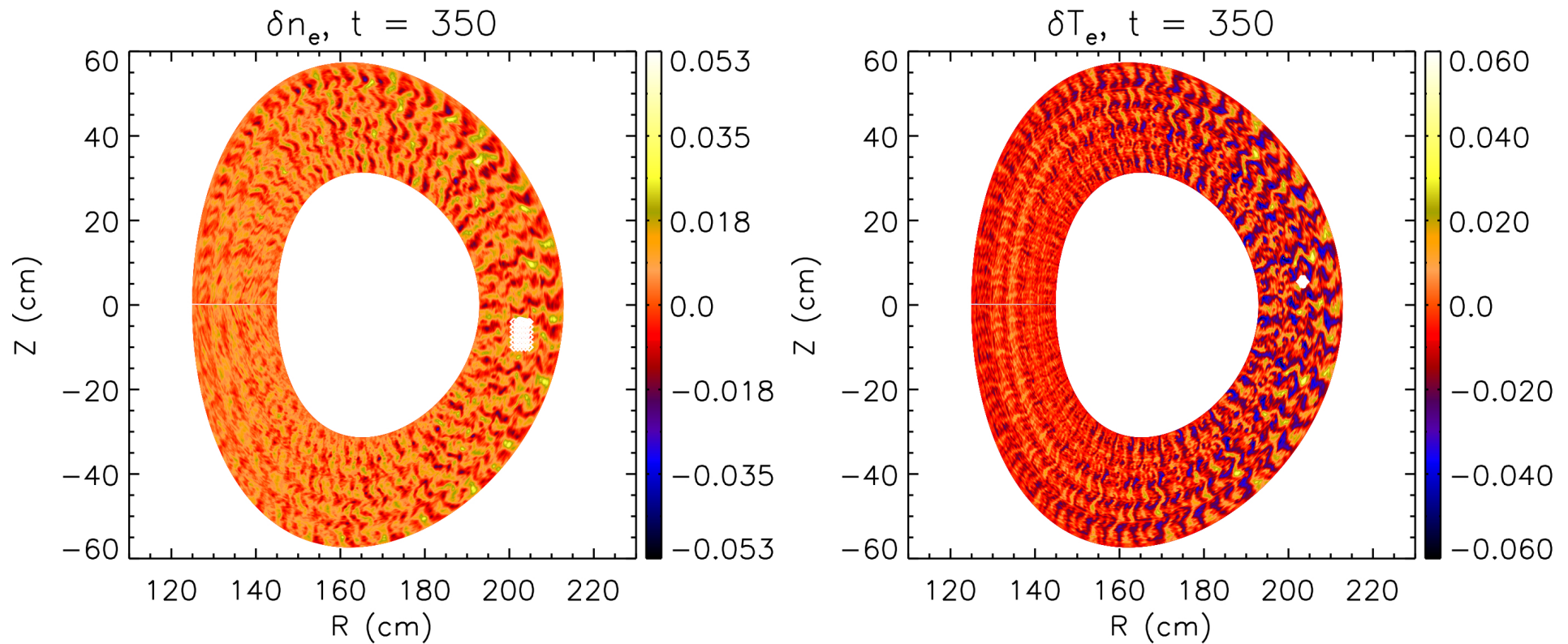
- At each time point of interest, record
 - Synthetic signal defined as

$$\delta n_{\text{synthetic}}(x, y, t) = \frac{\int d^2 x' \psi^{PSF}(x - x', y - y') \delta n_e^{GYRO}(x', y', t)}{\int d^2 x' \psi^{PSF}(x - x', y - y')}$$

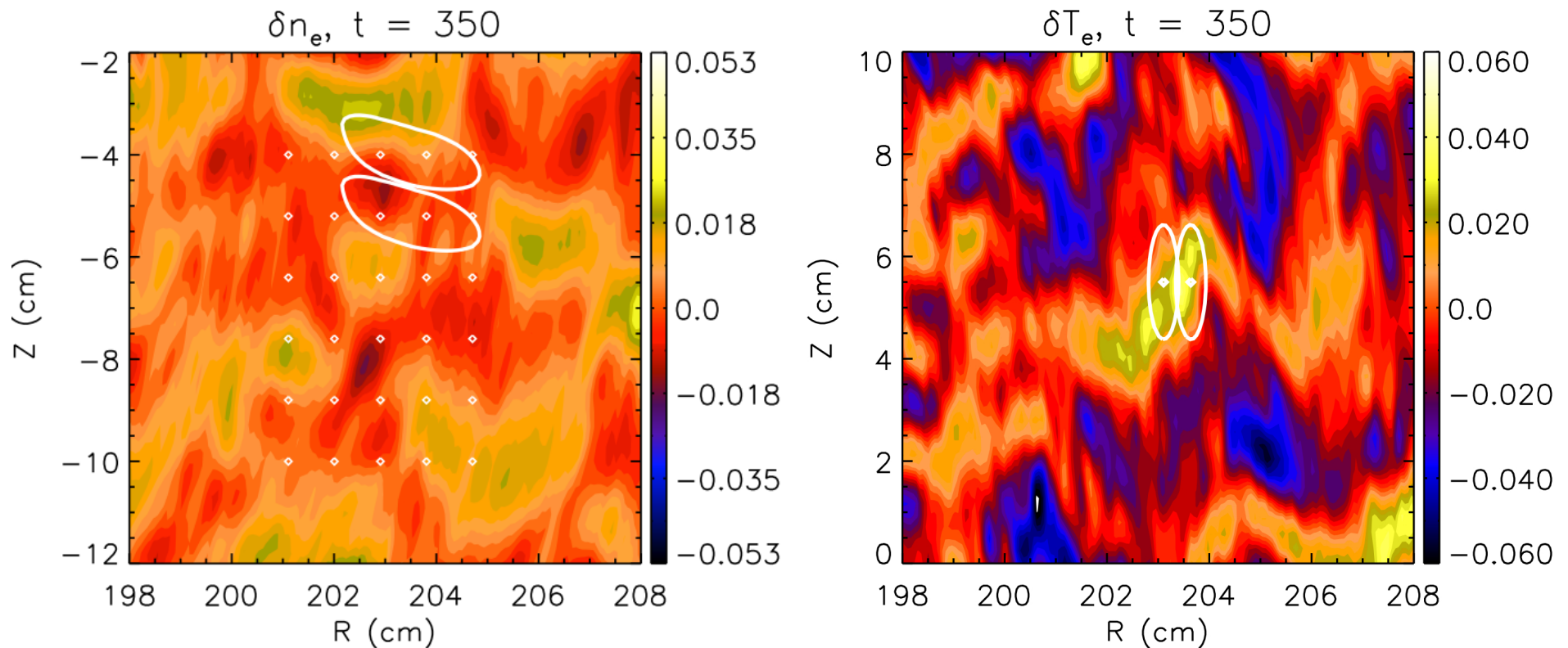
- GYRO signal at gridpoint closest to nominal BES location (term this signal the unfiltered GYRO signal in this poster)
- Because GYRO calculates fluctuations in co-rotating reference frame, must transform data back into the lab reference frame. Linear interpolation is used to increase the effective time resolution (equivalent to sampling rate) of the GYRO data, preventing aliasing due to the introduction of the equilibrium Doppler shift.



BES and CECE Fluctuation PSF Visualizations in (R,Z) Plane for $\rho = 0.5$ Simulation



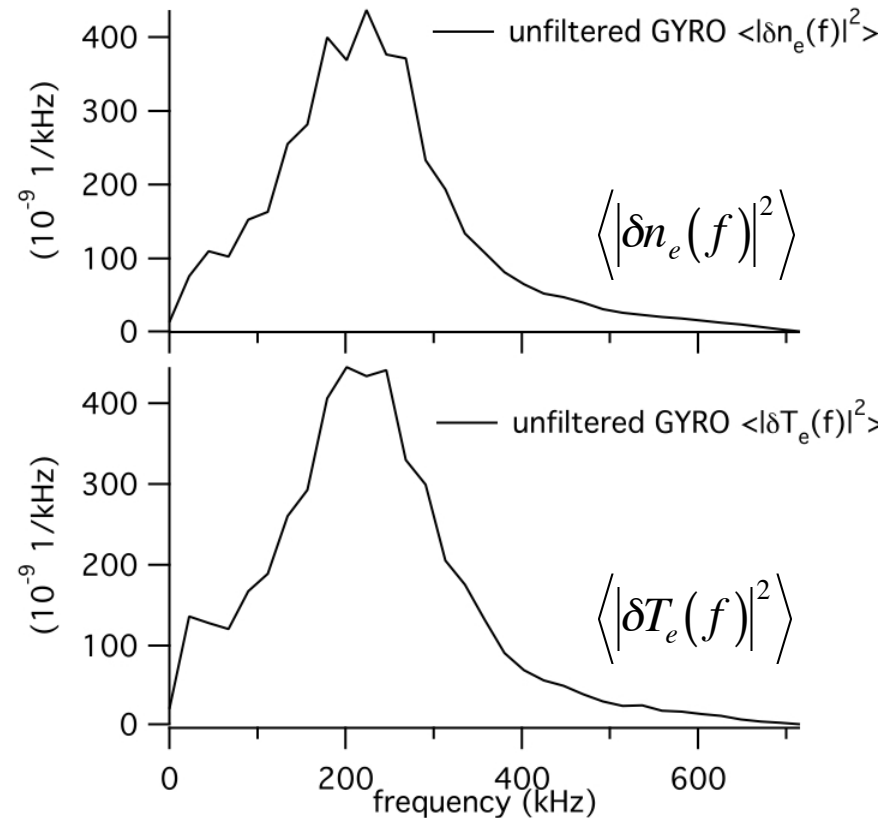
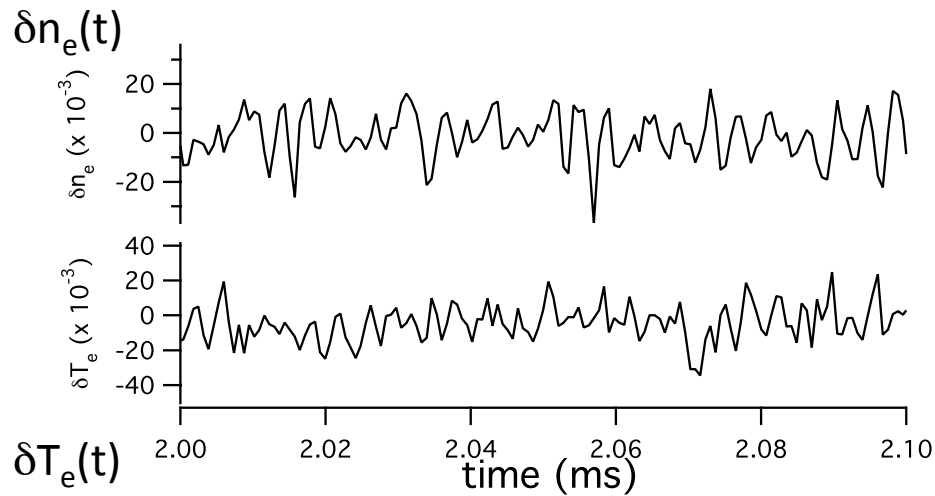
BES and CECE Fluctuation PSF Visualizations in (R,Z) Plane for $\rho = 0.5$ Simulation



50% contours of BES and CECE PSFs

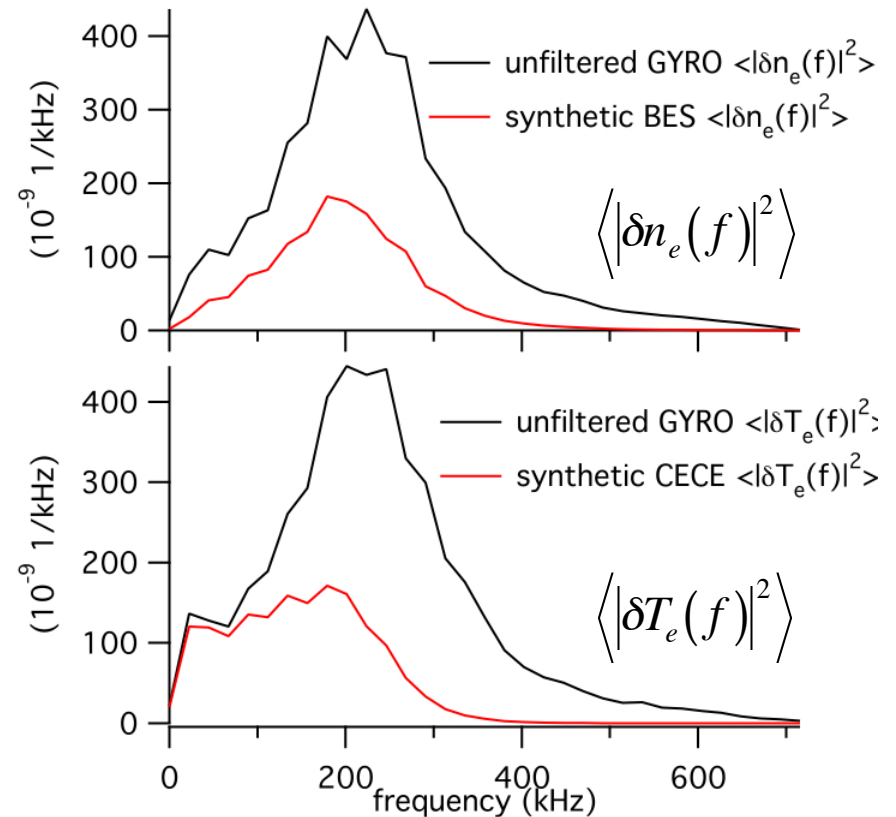
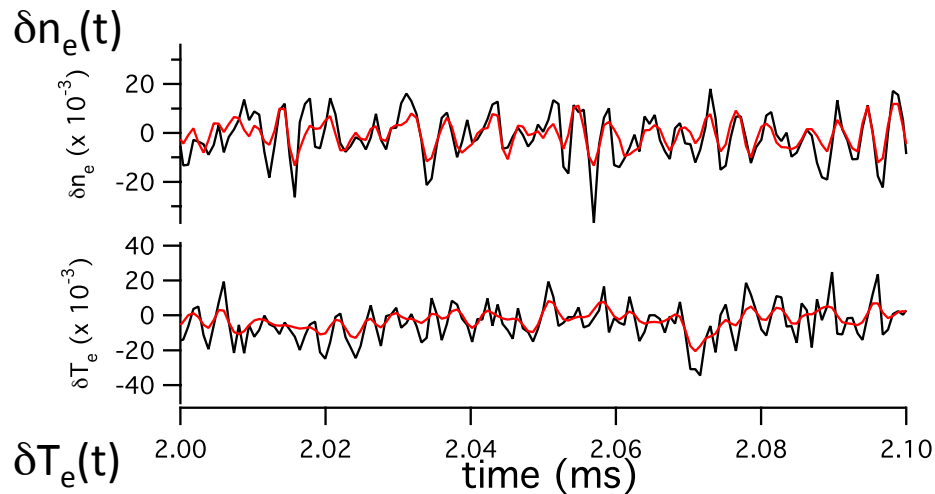
Synthetic Spectra Reflect Wavelength Sensitivities of Diagnostics

- Black is unfiltered GYRO



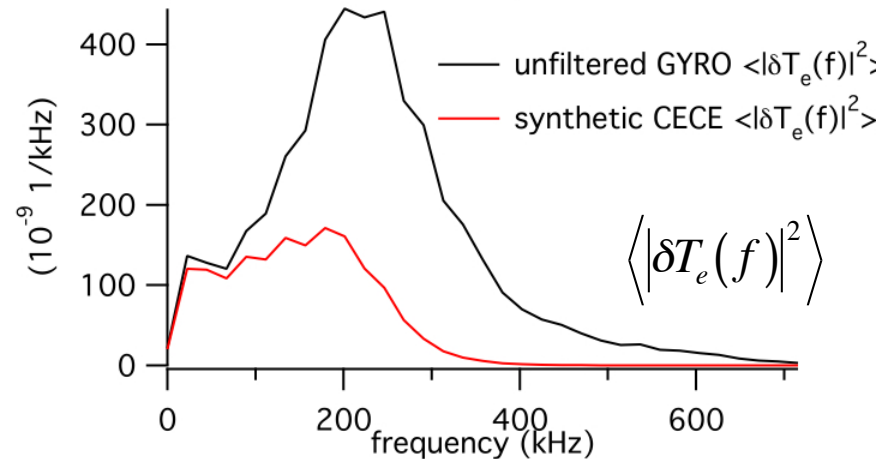
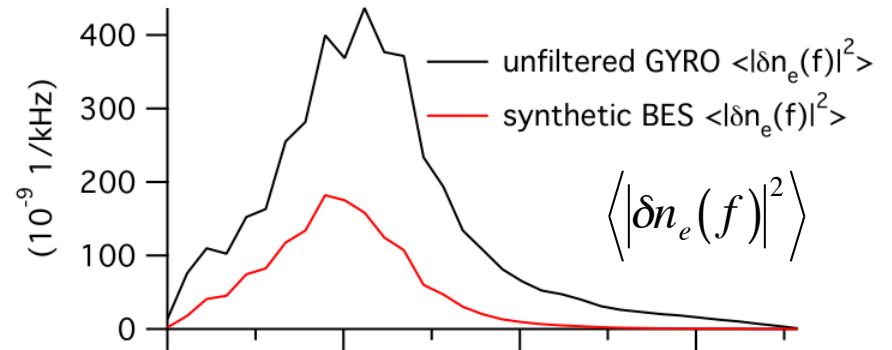
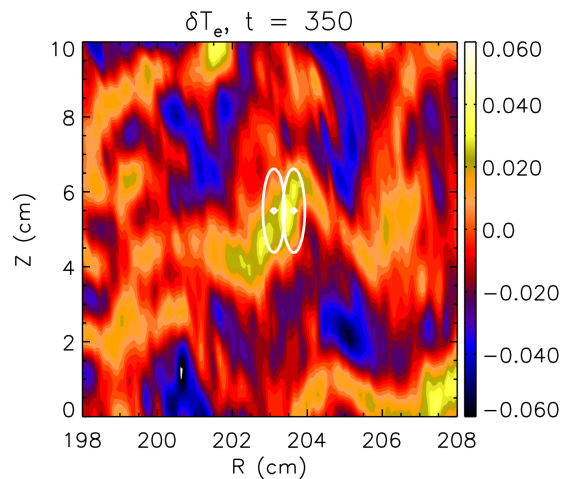
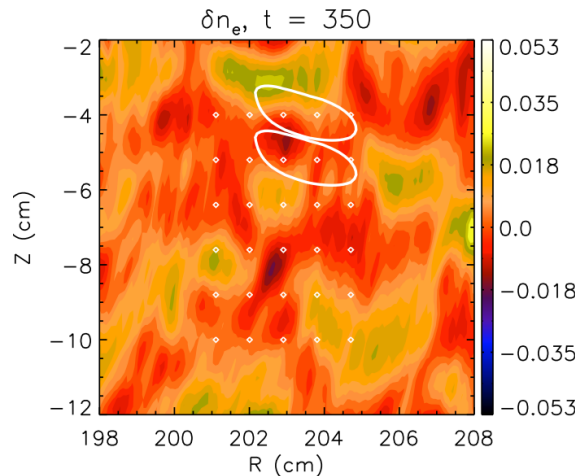
Synthetic Spectra of Both Diagnostics Exhibit Significant Attenuation

- Black is unfiltered GYRO, red is synthetic BES/CECE



Attenuation Frequency Dependencies Reflect Spatial Anisotropies of PSFs

- Large Doppler shift $\rightarrow f \sim k_z V_0$
- Leading BES PSF effect is to filter high $|k_R| \rightarrow$ weak frequency dependence
- Leading CECE PSF effect is to filter high $|k_z| \rightarrow$ strong frequency dependence

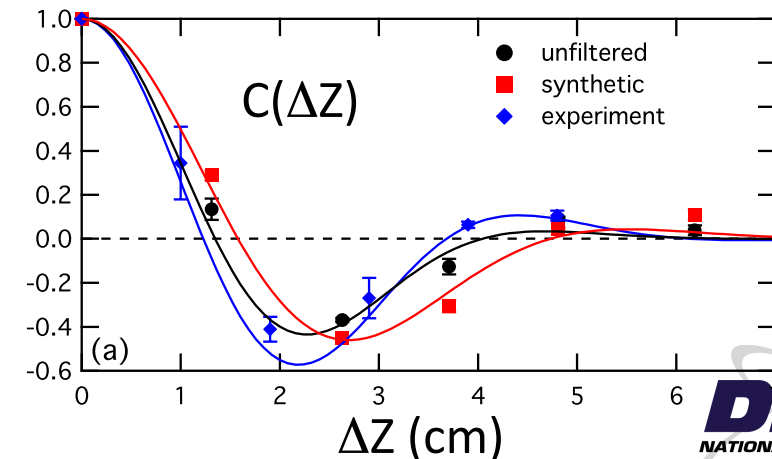
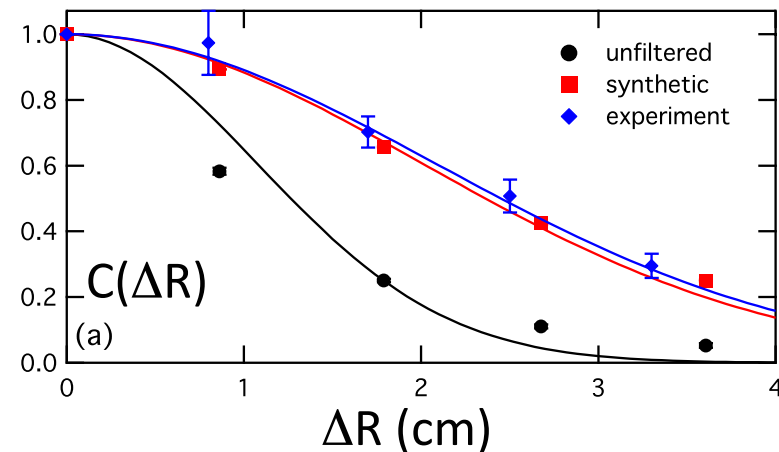


BES PSF Primarily Impacts Radial Correlation Length at $\rho = 0.5$

- Find good agreement between synthetic results and experiment for both radial and poloidal correlation length
 - Agreement in $C(\Delta Z)$ consistent with agreement in lab-frame power spectra
- Solid lines are Gaussians fit to **experimental BES**, synthetic BES and **unfiltered GYRO output** (fit gaussian*cos($k_0\Delta Z$) for $C(\Delta Z)$)

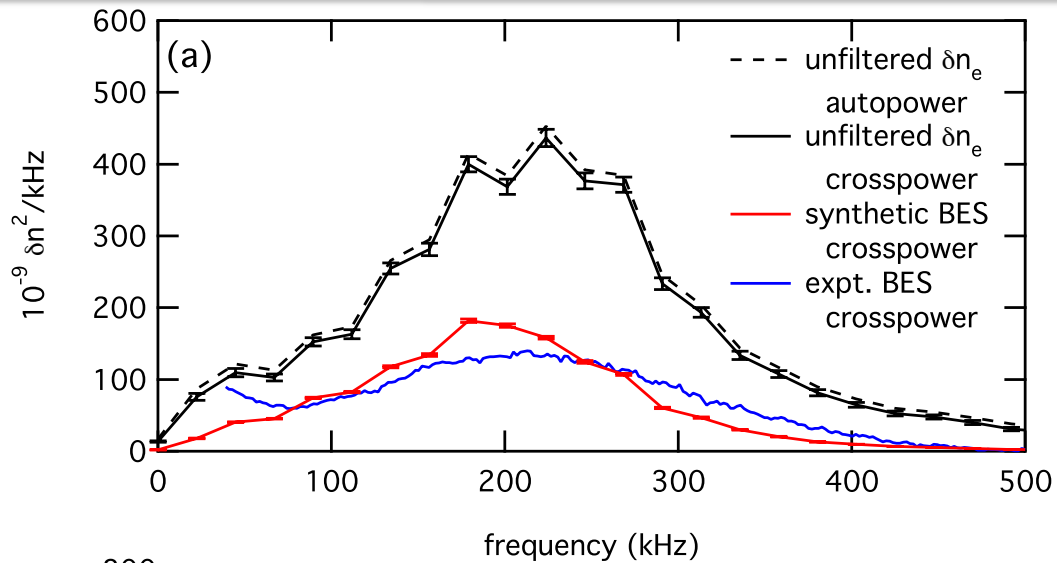
$$C(\Delta x) = \frac{\langle \tilde{n}(x,t) \tilde{n}(x + \Delta x, t) \rangle_t}{\sqrt{\langle |\tilde{n}(x,t)|^2 \rangle_t \langle |\tilde{n}(x + \Delta x, t)|^2 \rangle_t}}$$

	L_R (cm)	L_Z (cm)
GYRO (unfiltered)	1.5	2.7
Synthetic BES (all f)	2.8	3.3
Expt. BES (40-400 kHz)	2.9	3.1

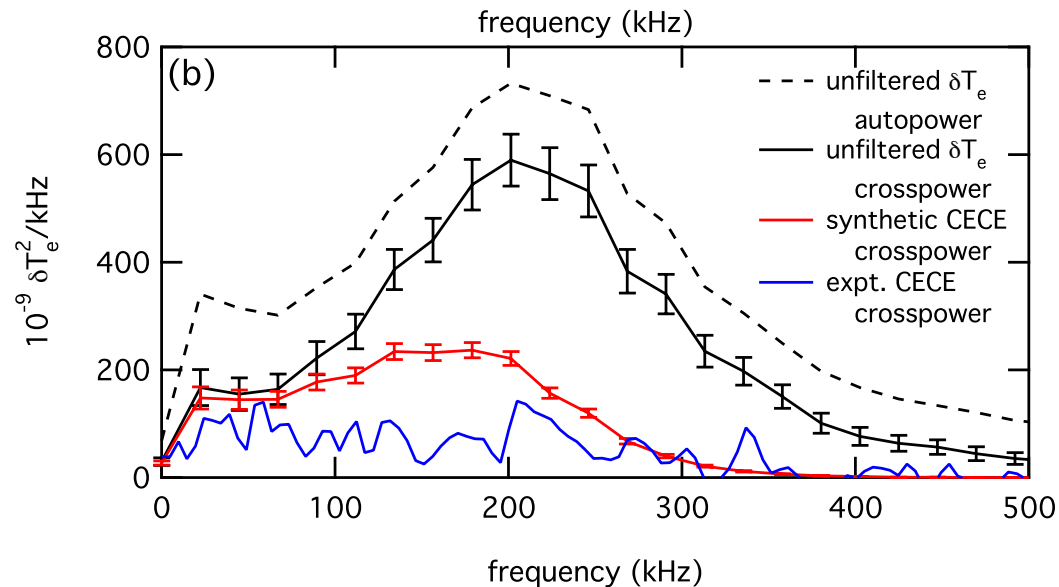


Lab-Frame Spectra Comparisons Show GYRO in Excellent Agreement with BES, but Overpredicting CECE

$$\langle |\delta n(f)|^2 \rangle$$

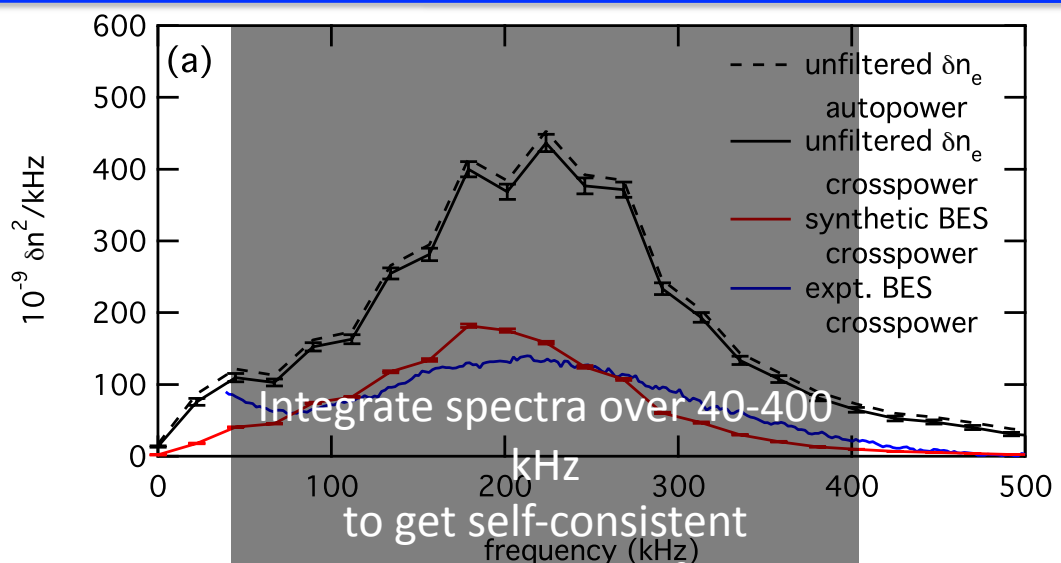


$$\langle |\delta T_e(f)|^2 \rangle$$

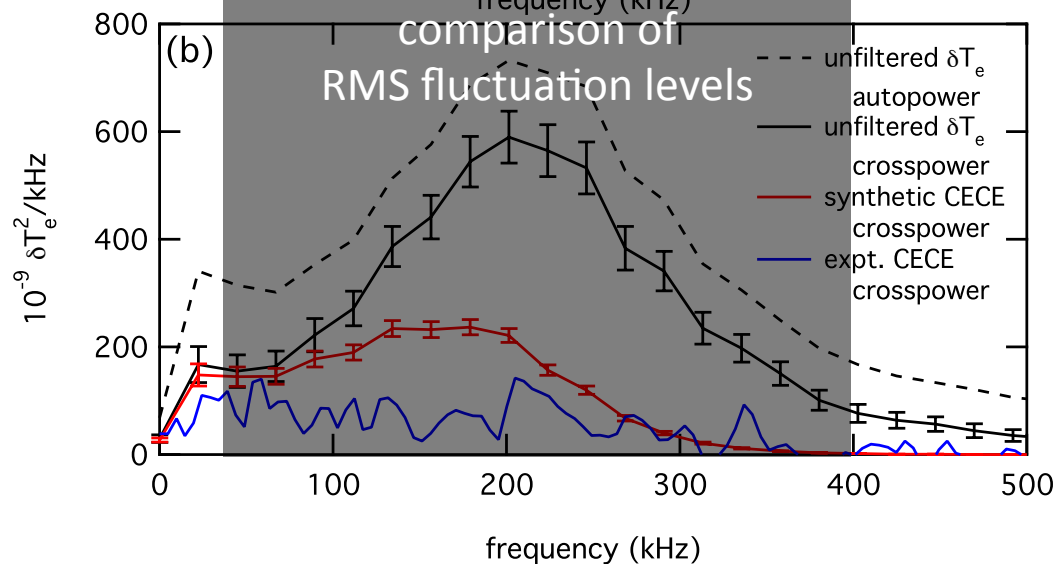


Lab-Frame Spectra Comparisons Show GYRO in Excellent Agreement with BES, but Overpredicting CECE

$$\langle |\delta n(f)|^2 \rangle$$



$$\langle |\delta T_e(f)|^2 \rangle$$



Quantifying RMS Fluctuation Levels at $\rho = 0.5$

- Fluctuation levels determined via: $\delta n_{RMS}^2 = \int_{40}^{400} df \left\langle \left| \delta n(f) \right|^2 \right\rangle$

GYRO RMS δn_e (autopower, all f)	1.0%	GYRO RMS δT_e (autopower, all f)	1.4%
---	-------------	---	-------------

Quantifying RMS Fluctuation Levels at $\rho = 0.5$

- Fluctuation levels determined via: $\delta n_{RMS}^2 = \int_{40}^{400} df \left\langle \left| \delta n(f) \right|^2 \right\rangle$

GYRO RMS δn_e (autopower, all f)	1.0%	GYRO RMS δT_e (autopower, all f)	1.4%
GYRO RMS δn_e (40 - 400 kHz)	$0.90\% \pm 0.015\%$	GYRO RMS δT_e (40-400 kHz)	$1.1\% \pm 0.057\%$

Quantifying RMS Fluctuation Levels at $\rho = 0.5$

- Fluctuation levels determined via: $\delta n_{RMS}^2 = \int_{40}^{400} df \left\langle \left| \delta n(f) \right|^2 \right\rangle$

GYRO RMS δn_e (autopower, all f)	1.0%	GYRO RMS δT_e (autopower, all f)	1.4%
GYRO RMS δn_e (40 - 400 kHz)	$0.90\% \pm 0.015\%$	GYRO RMS δT_e (40-400 kHz)	$1.1\% \pm 0.057\%$
syn. BES RMS δn_e (40 - 400 kHz)	$0.55\% \pm 0.0077\%$	syn. CECE RMS δT_e (40 - 400 kHz)	$0.66\% \pm 0.024\%$

Quantifying RMS Fluctuation Levels at $\rho = 0.5$

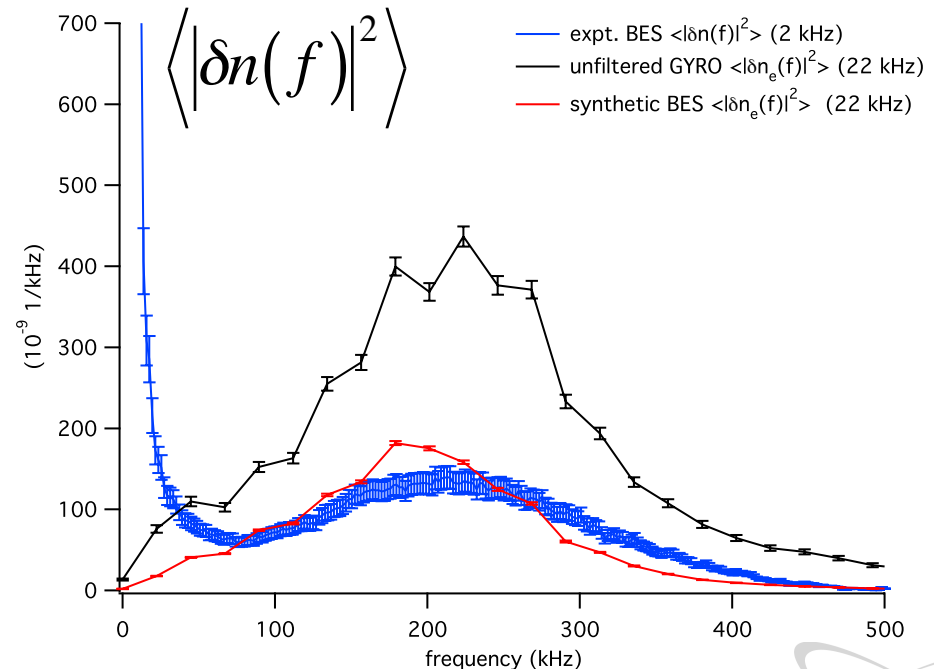
- Fluctuation levels determined via: $\delta n_{RMS}^2 = \int_{40}^{400} df \left\langle \left| \delta n(f) \right|^2 \right\rangle$

GYRO RMS δn_e (autopower, all f)	1.0%	GYRO RMS δT_e (autopower, all f)	1.4%
GYRO RMS δn_e (40 - 400 kHz)	$0.90\% \pm 0.015\%$	GYRO RMS δT_e (40-400 kHz)	$1.1\% \pm 0.057\%$
syn. BES RMS δn_e (40 - 400 kHz)	$0.55\% \pm 0.0077\%$	syn. CECE RMS δT_e (40 - 400 kHz)	$0.66\% \pm 0.024\%$
expt. BES RMS δn (40-400 kHz)	$0.56\% \pm 0.1\%$	expt. CECE RMS δT_e (40-400 kHz)	$0.4\% \pm 0.2\%$

One swindle: Different Frequency Resolutions Used for Synthetic and Experimental Spectra

- Swindle: used low freq resolution (22 kHz) for syn. diagnostics, vs 2 kHz for expt.
 - BES spectrum plotted with 10% uncertainty

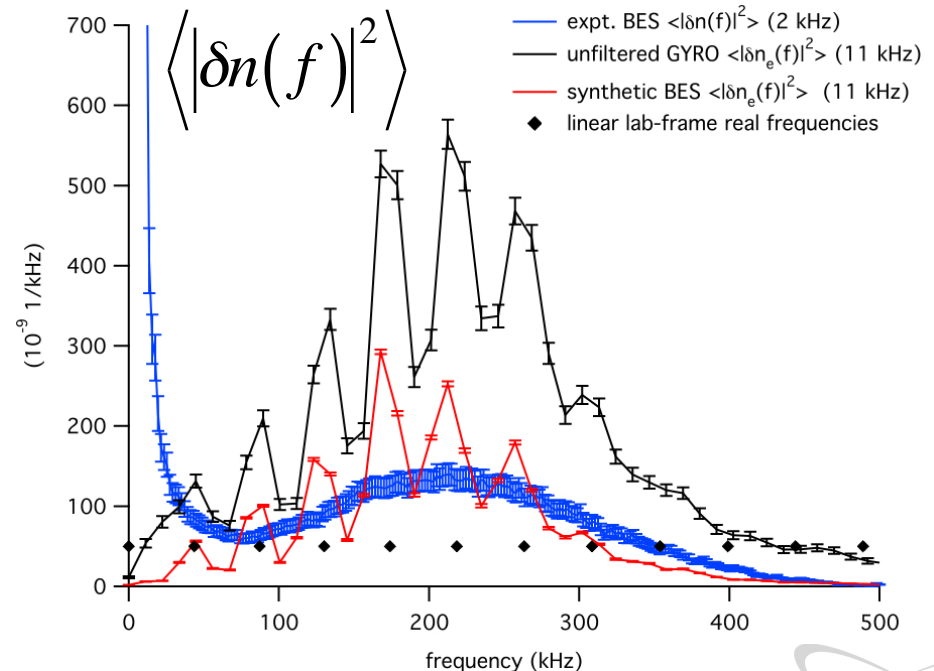
	RMS δn (40 - 400 kHz)
Expt. (2.5 kHz)	0.56
Sim (22 kHz)	0.55



Increased Frequency Resolution Brings Out Finite Δn Structure of Synthetic Signals

- Swindle: used low freq resolution (22 kHz) for syn. diagnostics, vs 2 kHz for expt
- If we calculate synthetic spectra with double freq resolution, observe features well-correlated with discrete n values
 - Features robust with even higher resolution, but SNR decreases quickly

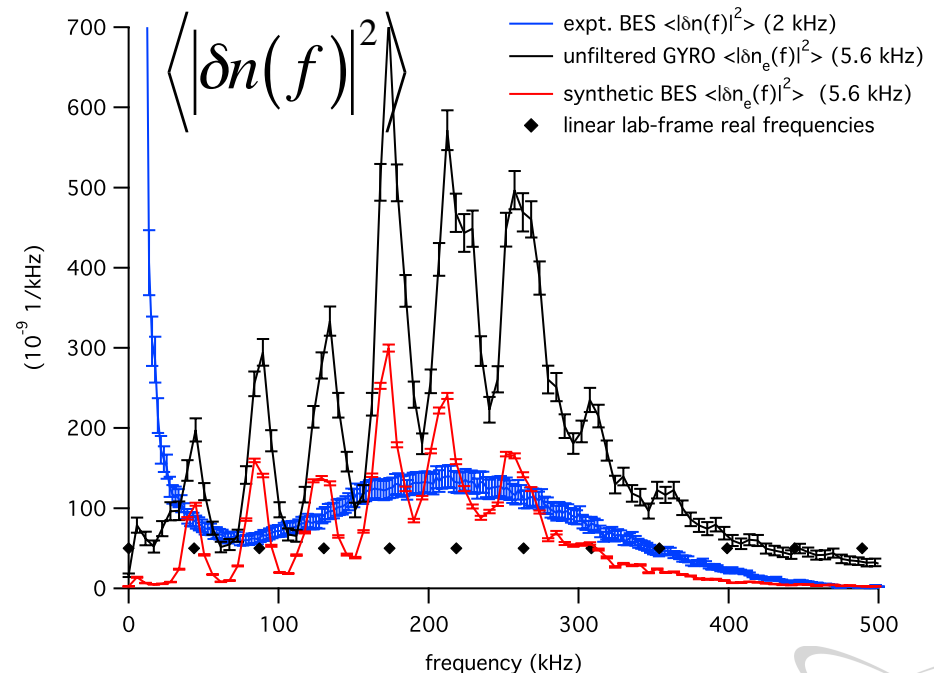
	RMS δn (40 - 400 kHz)
Expt. (2.5 kHz)	0.56
Sim (22 kHz)	0.55
Sim (11 kHz)	0.58



Increased Frequency Resolution Brings Out Finite Δn Structure of Synthetic Signals

- Swindle: used low freq resolution (22 kHz) for syn. diagnostics, vs 2 kHz for expt
- If we calculate synthetic spectra with double freq resolution, observe features well-correlated with discrete n values
 - Features robust with even higher resolution, but SNR decreases quickly

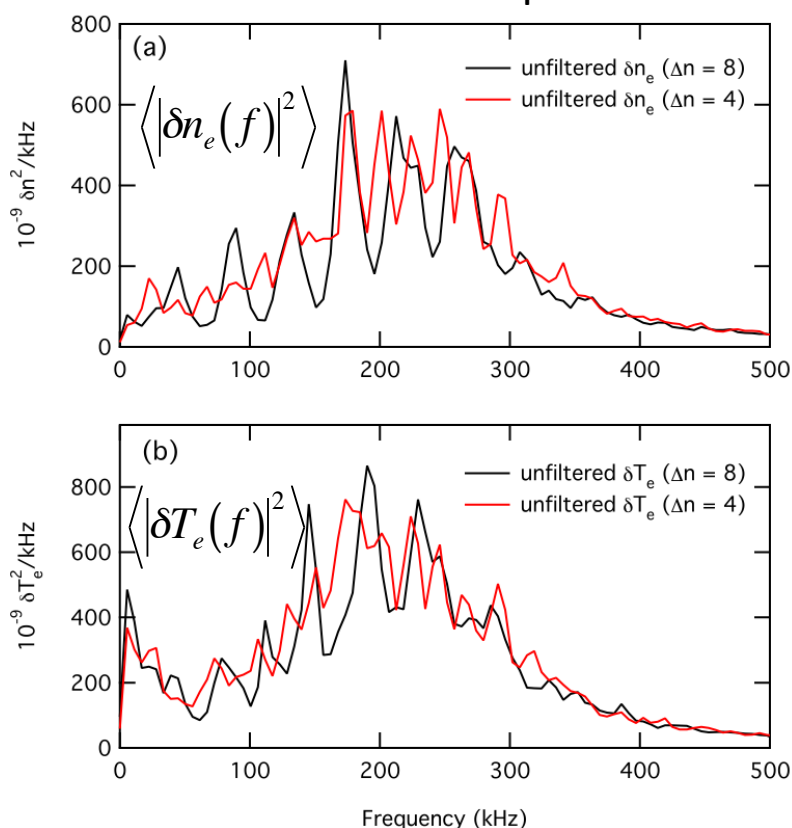
	RMS δn (40 - 400 kHz)
Expt. (2.5 kHz)	0.56
Sim (22 kHz)	0.55
Sim (11 kHz)	0.58
Sim (5.6 kHz)	0.56



Using $\Delta n=4$ Gives Same Integrated Values as $\Delta n = 8$ with Smoother Lab-Frame Power Spectra but Same Transport

- For concreteness, compare spectra from **32-mode simulation with $\Delta n=4$** against 16-mode simulation with $\Delta n=8$
 - Corresponds to BOUT.inp: ZPERIOD = 4 vs. ZPERIOD = 8 & doubling MZ

Unfiltered GYRO spectra



	16 modes	32 modes
χ_i / χ_{gB}	1.1 ± 0.2	1.1 ± 0.1
χ_e / χ_{gB}	1.0 ± 0.2	1.0 ± 0.1

Initial BOUT++ simulations of D3D L-mode edge predict fluctuations qualitatively consistent with BES and probe measurements
[B. I. Cohen *et al.*, Phys. Plasmas **20** 055906 (2013)]

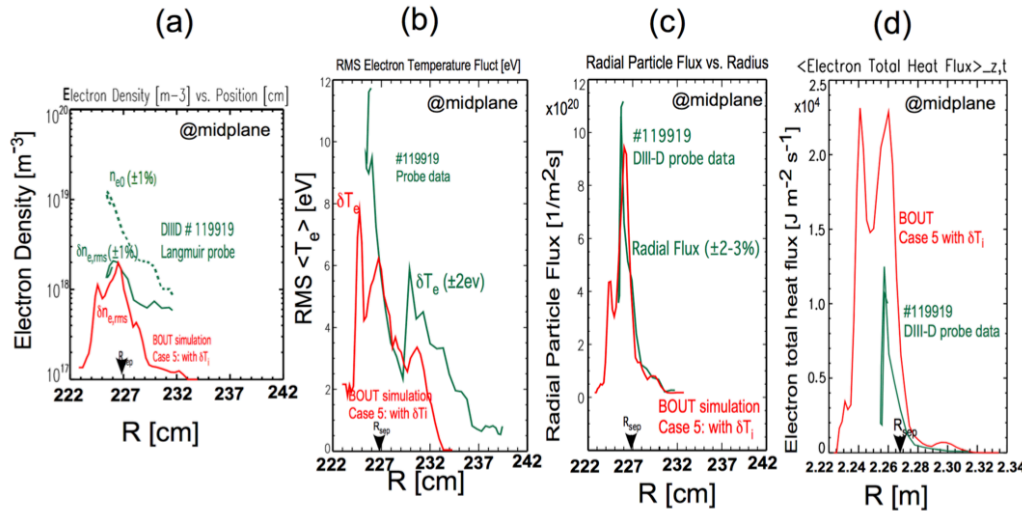


FIG. 7. Comparison to probe data (green) to case 5 simulation (red) of shot #119 919 for (a) electron density and (b) electron temperature fluctuations, (c) radial particle flux, and (d) total electron radial heat flux vs. probe radius position at the midplane.

- Comparisons to BES use an analytic PSF, but still observe significant differences between filtered and unfiltered signals

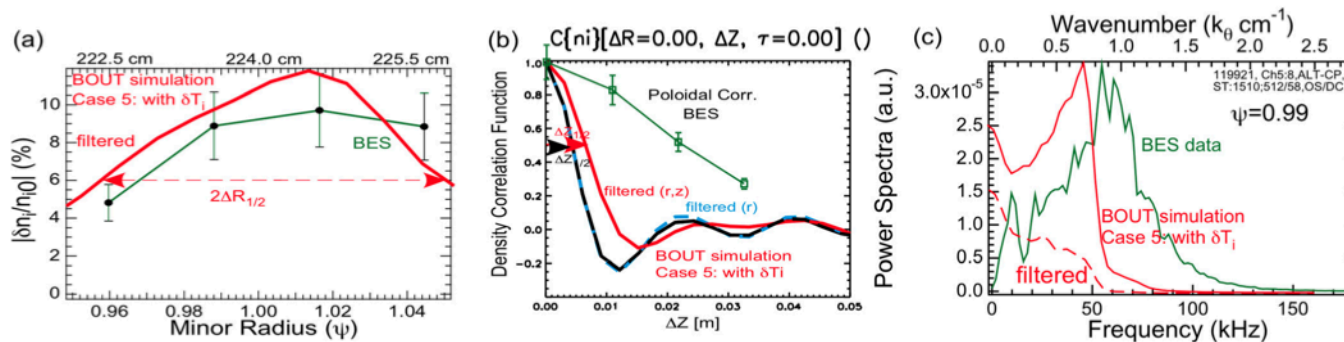


FIG. 8. Shot #119 919. Comparison of BES data (green) to synthetic diagnostics for case 5 simulation (red) for (a) relative electron density vs. radius near midplane, (b) density correlation function vs. Δz separation, and (c) density fluctuation power spectrum vs. frequency.

Initial Synthetic Langmuir Probe Studies Find T_e Fluctuations Can Significantly Impact V_{float} Results

[B. Nold *et al.*, New J. Phys **14** 063002 (2012)]

- Langmuir probes measure floating potential V_{float} and ion saturation current I_{sat} which are related to plasma quantities via sheath relationships such as

$$I_{sat} = 0.61 A_{probe} e n_e \sqrt{\frac{k_b (T_e + T_i)}{m_i}}$$

$$V_{float} = V_{plasma} - \Lambda \frac{k_b T_e}{e}, \quad \Lambda \approx 3$$

- Applying these relationships to a GEMR fluid edge simulation, Nold *et al* find I_{sat} tracks n_e well, but V_{float} and V_{plasma} have significantly phase shift
- Need to understand how this translates into particle flux, Reynolds stress measurements
- Also see P. Ricci *et al.*, PoP **16** 055703 (2009) for very good synthetic Langmuir probe validation study

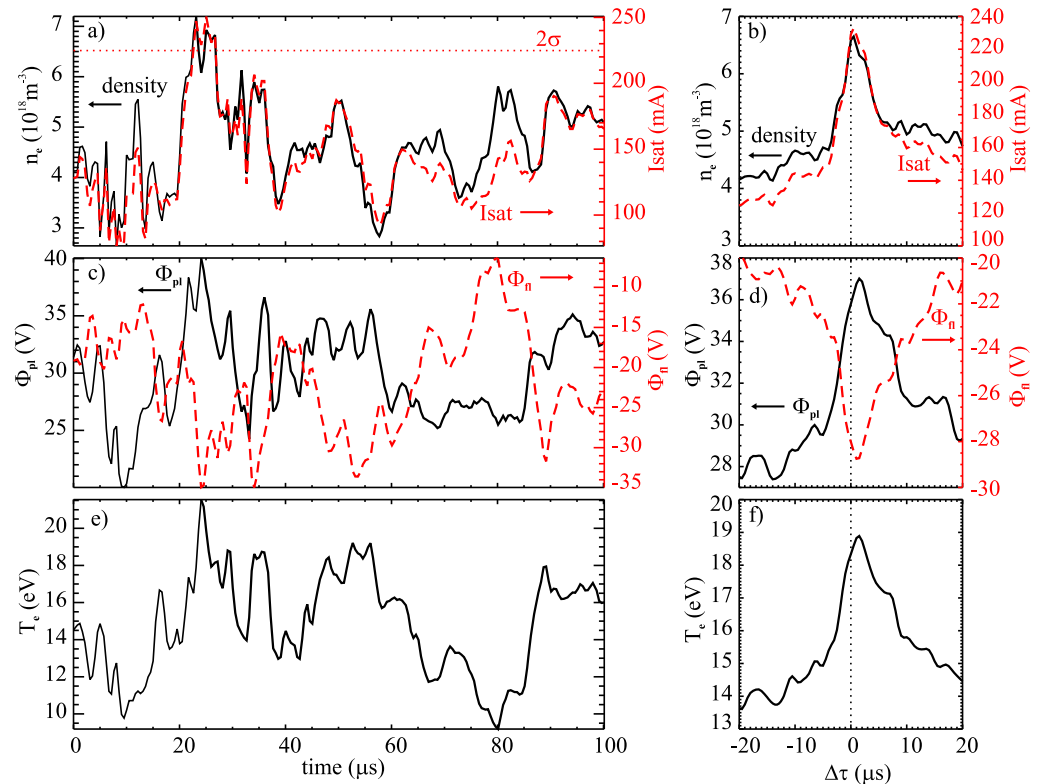


Figure 4. Comparison of measured plasma fluctuations from emissive and non-emissive Langmuir probes in the SOL of ASDEX Upgrade. Detail of time series (left) and conditionally averaged fluctuations (right). Top: density and ion-saturation current (dashed); middle: plasma and floating (dashed) potentials; bottom: electron temperature from equations (5) and (6).

Synthetic Gas-Puff Imaging Applied SOLT Simulations of NSTX L-mode Consistent with Experiment

[D. A. Russell *et al.*, Phys. Plasmas **18** 022306 (2011)]

- Calculate a synthetic intensity $I = N_o * f_A(n_e, T_e)$, where N_o is gas puff density (obtained from separate DEGAS2 simulation) and f_A is a tabulated atomic emission function

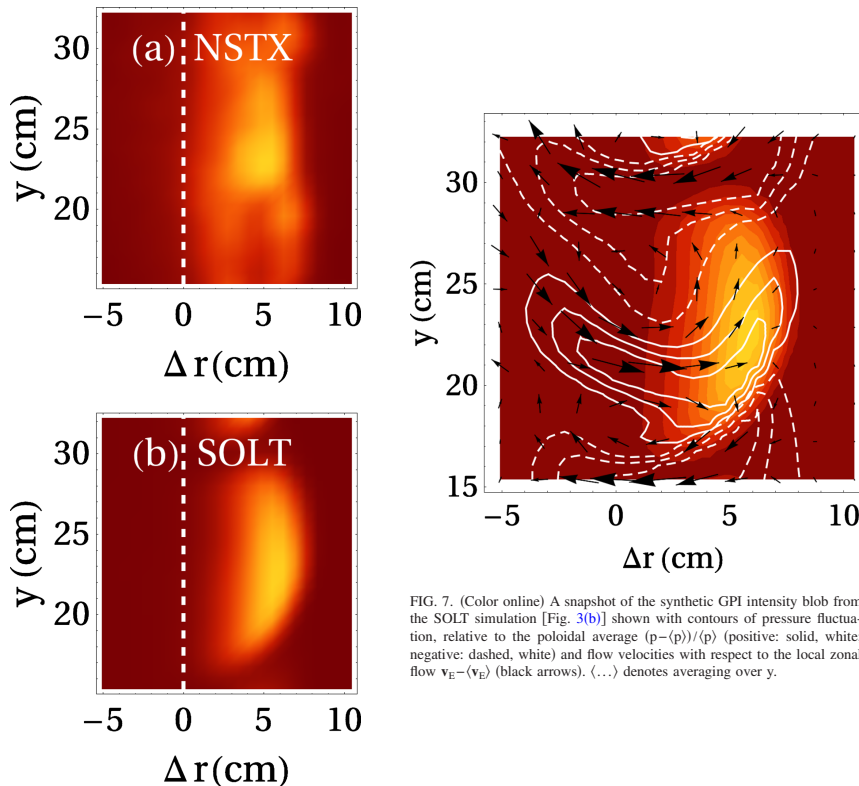


FIG. 3. (Color online) (a) Actual (NSTX, shot no. 112825) and (b) synthetic SOLT GPI intensity images. The magnetic separatrix is at $\Delta r = 0$ in the NSTX shot. Intensities are normalized by their respective global maxima over the frame. The SOLT window is a subdomain ($\sim 1/9$) of the full simulation ($\beta = 1.75 \times \beta_0$).

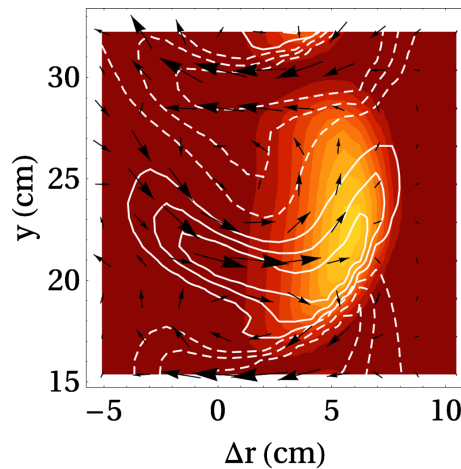


FIG. 7. (Color online) A snapshot of the synthetic GPI intensity blob from the SOLT simulation [Fig. 3(b)] shown with contours of pressure fluctuation, relative to the poloidal average $(p - \langle p \rangle) / \langle p \rangle$ (positive: solid, white; negative: dashed, white) and flow velocities with respect to the local zonal flow $v_E - \langle v_E \rangle$ (black arrows). (...) denotes averaging over y .

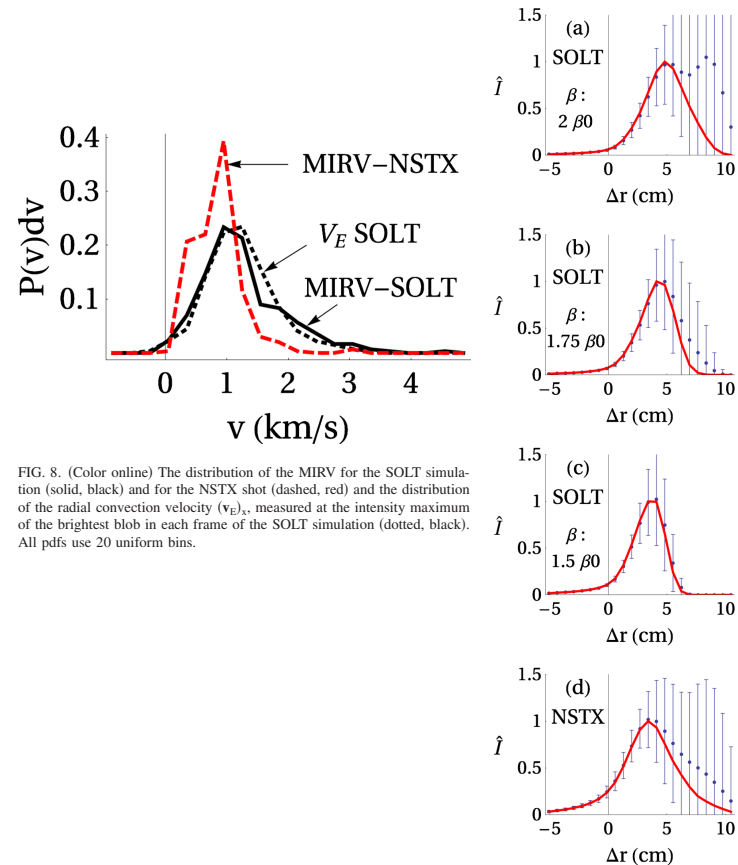


FIG. 8. (Color online) The distribution of the MIRV for the SOLT simulation (solid, black) and for the NSTX shot (dashed, red) and the distribution of the radial convection velocity $(v_E)_y$, measured at the intensity maximum of the brightest blob in each frame of the SOLT simulation (dotted, black). All pdfs use 20 uniform bins.

FIG. 4. (Color online) Median (solid, red) and average (dots) GPI intensities, sampled over y and t (300 frames), vs radius for three drive strengths in the SOLT simulations (a) $\beta = 2 \times \beta_0$, (b) $\beta = 1.75 \times \beta_0$, and (c) $\beta = 1.5 \times \beta_0$, compared to (d) the GPI camera data for NSTX shot no. 112828. Error bars denote root-mean-square deviation from the average. All data are normalized to the maximum value of the median in each case.

Take-away points

- Synthetic diagnostics represent a crucial step in performing quantitative (and sometimes even qualitative) code-experiment comparisons
- Implementing a synthetic diagnostic is actually fairly easy. Implementing a good synthetic diagnostic requires close coupling with relevant diagnostic group to get accurate and complete incorporation of relevant physics
- Edge simulations like BOUT have many possibilities for impactful research in this area.